Acetyl group orientation modulates the electronic ground-state asymmetry of the special pair in purple bacterial reaction centers

Wawrzyniak, P.K.; Beerepoot, M.T.P.; Groot, H.J.M. de; Buda, F.

PCCP

Cite this: *Phys. Chem. Chem. Phys.*, 2011, **13**, 10270–10279

www.rsc.org/pccp

PAPER

Acetyl group orientation modulates the electronic ground-state asymmetry of the special pair in purple bacterial reaction centers

P. K. Wawrzyniak, M. T. P. Beerepoot, H. J. M. de Groot and F. Buda*

Received 24th January 2011, Accepted 28th March 2011
DOI: 10.1039/c1cp20213h

Recent experimental data point to an asymmetric ground-state electronic distribution in the special pair (P) of purple bacterial reaction centers, which acts as the primary electron donor in photosynthesis. We have performed a density functional theory investigation on an extended model including the bacteriochlorophyll dimer and a few relevant surrounding residues to explore the origin of this asymmetry. We find strong evidence that the ground-state electron density in P is intrinsically asymmetric due to protein-induced distortions of the porphyrin rings, with excess electron charge on the P_M bacteriochlorophyll cofactor. Moreover, the electron charge asymmetry is strongly modulated by the specific orientation of the $C3^1$ acetyl group, which is hydrogen bonded to His168. The electronic excitation has a significant charge transfer character inducing a displacement of electron charge from P_L to P_M, in agreement with experimental data in the excited state. These results are relevant for the understanding of the unidirectional electron transfer path in photosynthesis.

1. Introduction

One essential process in photosynthesis is the photo-induced charge separation taking place in the photosynthetic reaction center membrane protein.[1] The elucidation of the 3D structure of purple bacteria reaction centers (PBRCs) has been a crucial step for mechanistic studies of photosynthesis.[2] The X-ray structures of various PBRCs have revealed that the L- and M-polypeptides and associated cofactors are arranged in two nearly symmetric membrane-spanning branches (L-branch and M-branch). Despite the apparent structural symmetry of the reaction center, spectroscopic studies have shown that only one of the two potential electron-transfer chains, the so-called L-branch, is active in catalyzing the electron transfer.[3] The primary electron donor is the so-called special pair (P), a dimer of bacteriochlorophylls *a* (BChl's *a*), which will be indicated in the following as P_L and P_M. Photoexcitation of P with red or near-infrared light to its lowest singlet excited state (P*) triggers electron transfer across the membrane to the ubiquinone Q_A *via* a monomeric BChl *a* (B_A) and a bacteriopheophytin, BPhe (H_A).[4] It has been also shown that excitation with blue light into the Soret band of PBRC gives rise to electron transfer along the alternate branch.[5] In this case however, the special pair P is not involved in the early stage of the photochemistry and the electron donor appears to be the monomeric BChl (B_B).

Leiden Institute of Chemistry, Leiden University, P.O. Box 9502, 2300 RA Leiden, The Netherlands.
E-mail: f.buda@chem.leidenuniv.nl; Fax: +31 (0)71 5274603; Tel: +31 (0)71 5275723

Electronic asymmetry in the special pair (P) of PBRC is believed to affect the directionality of the electron transfer process and has been therefore much studied.[6–10] The EPR and ENDOR studies for the cation radical $P^{\bullet +}$ have shown a disproportion in spin density distribution in favor of P_L.[6,11–13] From the Stark experiments on the excited state P* on the other hand, it has been proposed that more electron density is concentrated on P_M.[14] It has been also reported that in the ground state there is an excess negative charge located on P_L.[8,15] Recently, a suggestion has been made from photo-CIDNP solid-state NMR experiments that the asymmetry, both in the electronic ground-state and in the radical cation state, is caused by an intrinsic property of the special pair supermolecule, which is attributable to a modification of the structure of P_L.[16] Moreover, differences in electronic density distribution between ground-state and radical state have been explained by polarization effects due to the His L168 hydrogen bonded to the 3^1 acetyl group of P_L (see Scheme 1 for the atomic labeling).[8,16] However, the electrostatic interactions within the bacteriochlorophylls *a* (BChl *a*) in the special pair and with the protein environment can also play an important role in determining the structure and electronic distribution of P.[17] This has been recently shown by Ganapathy and coworkers for the Zinc chlorin aggregates, where it was found that the self-assembly can be driven mostly by electrostatic and van der Waals interactions without hydrogen bonding.[18] Also recent theoretical investigations on the cation radical state of the special pair suggest that electronic asymmetry may be associated with different orientations of the phytyl tails and the methyl ester group on the $C13^2$ carbon atoms.[9,10]

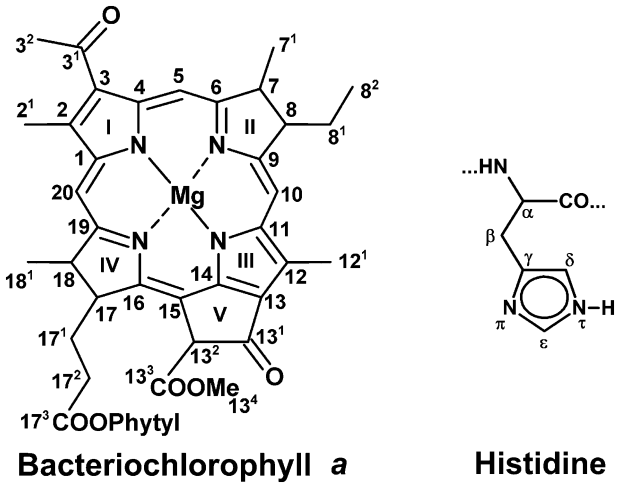

Scheme 1 Schematic representation of the bacteriochlorophyll *a* and histidine structures with the corresponding atomic labeling used throughout the paper.

Given that a detailed and consistent picture on the origin of the electronic asymmetry has not emerged yet, in this paper we investigate how the electronic density in the ground-state is influenced by different structural properties of the special pair bacteriochlorophylls *a* and by their interaction with axial histidines and other neighboring residues. A particularly interesting aspect is the orientation of the P_L 3^1 acetyl group, which in the 1PCR[19] crystal structure is substantially different from all the other *Rb. sphaeroides* RC structures deposited in the Protein Structure Database. This orientation can be characterized by the C4–C3–$C3^1$–$O3^1$ dihedral angle (φ_{ac}), which equals 88° for the 1PCR structure and ranges between −2° and 21° for all the others.[20] This large difference makes the 1PCR crystal structure somewhat special and thus interesting to compare with other structures such as, for example, the 1QOV structure,[21] where the dihedral angle is 13°, almost in the middle of the observed range. Fine details of the X-ray structures, such as the orientation of the acetyl group, may be affected by the resolution in the crystallographic data and by the models used in the refinement. Density Functional Theory (DFT) calculations can help in these cases by providing further insight in the optimal geometry beyond simple force-field models. It turns out that the orientation of the 3^1 acetyl group of P_L BChl *a*, which depends on the hydrogen bond with His L168, is crucial for the electronic density distribution among the two P_L and P_M bacteriochlorophylls *a*. In this way the protein can tune the biophysical properties of the special pair by inducing conformational changes to the acetyl and therefore to the strength of conjugation with the porphyrin π system. Finally, we study the effects of the neighboring residues on the absorption properties of bacteriochlorophylls *a* and show how the localization of the molecular orbitals relevant for the Q_y excitations strongly depends on the structural properties of the BChls *a* in the special pair.

2. Models and methods

Density Functional Theory (DFT) calculations were performed using the ADF computational code[22–24] with the BLYP[25–27] functional and the TZP Slater type basis set. The initial model, extracted from the 1PCR crystal structure of *Rhodobacter sphaeroides* bacterial reaction center,[19] included the special pair, the two axial histidines (His L173 and His M202), two water molecules (HOH 1007 on the L-side and HOH 1051 on the M-side) and the aminoacid residues His L168, Asn L166 and Phe M197. The phytyl side chains of bacteriochlorophylls *a* were truncated to a methyl group and broken peptide bonds were saturated to a neutral amino acid termination (COOH–NH2).

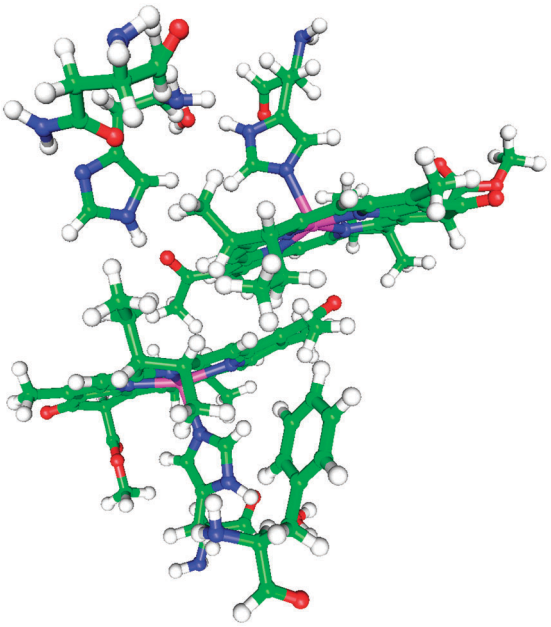

Fig. 1 Ball and stick representation of model **8**, the largest model considered in this study containing approximately 250 atoms.

In order to remove experimental uncertainties, the initial model was partially optimized by relaxing carbons and nitrogens in the porphyrin ring, and all the hydrogen atoms (model **8**, see Fig. 1). In this way the X-ray crystallography errors and molecular modelling refinement artifacts were corrected by DFT, while preserving the supramolecular structure of the system due to the applied constraints. Subsequently, a series of models were built by cutting the partially optimized model into separate fragments. For an overview see Fig. 2. Additionally, the models **5** and **6** were partially optimized, relaxing in each of them the two imidazole rings of the axial histidines and the two magnesium atoms.

To investigate the impact of the 3^1 acetyl group rotation, the special pair in model **1** was used as a starting point to create two models: **9** and **10**. In the model **10**, the P_L acetyl was additionally rotated to mimic the P_M acetyl orientation. Subsequently, the geometry of the P_L acetyl group was relaxed in both models **9** and **10**, by optimizing the positions of $C3^1$, $O3^1$ and the $C3^2$ methyl group. This procedure has been used extensively in the past for the description of the relation between the functional electronic structure and the geometry of a ligand bound to its membrane protein partner.[28]

Finally, P_L and P_L + His L168 were extracted from model **1** to form models **13** and **14**, respectively. In both of these models the acetyl group of P_L was relaxed by optimizing

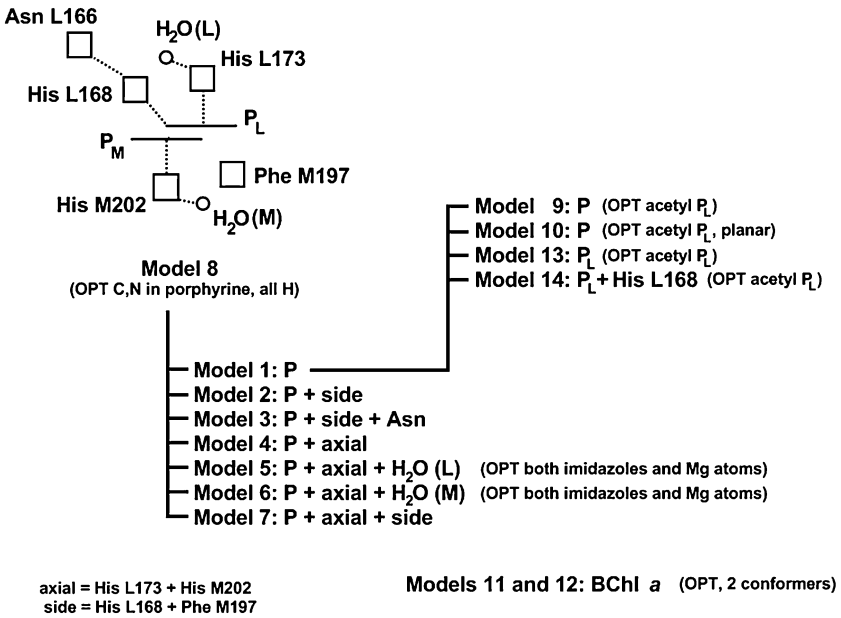

Fig. 2 An overview of theoretical models used in this work. Model **8** is also shown schematically here.

geometrical positions of $C3^1$, $O3^1$ and the $C3^2$ methyl group. Additionally two fully optimized bacteriochlorophyll *a* molecules were constructed with different orientations of the acetyl group: one in which the $C3^2$ methyl group points towards the $C2^1$ methyl (model **11**) and one in which the oxygen points towards the $C2^1$ methyl (model **12**).

The quadrupole derived charge analysis was performed as implemented in the ADF.[29] Electron density difference maps were calculated by subtracting from the electronic density of a model, the electronic densities of its fragments. The excitation energies were calculated using TDDFT/TZP with the "Statistical Averaging of Orbital Potentials" (SAOP) potential,[30–32] which is well-suited for molecular response properties.

3. Results and discussion

3.1 Asymmetry of the special pair

The total quadrupole derived charges for P_L and P_M in the various models described above are presented in Table 1. For the model **1** comprising the special pair only, an electronic asymmetry is found, with P_M having an excess of 0.16 electron charge compared to P_L bacteriochlorophylls *a*. Thus, the asymmetry appears to be an intrinsic feature of P, at least within the model derived by the 1PCR structural data. Addition of the two side residues, His L168 and Phe M197 (model **2**) has only a minor effect on the electron density of P with a small decrease in the positive charge of P_L. One would expect that due to the hydrogen bond with the histidine His L168, the 3^1 acetyl would donate electron charge, thus making

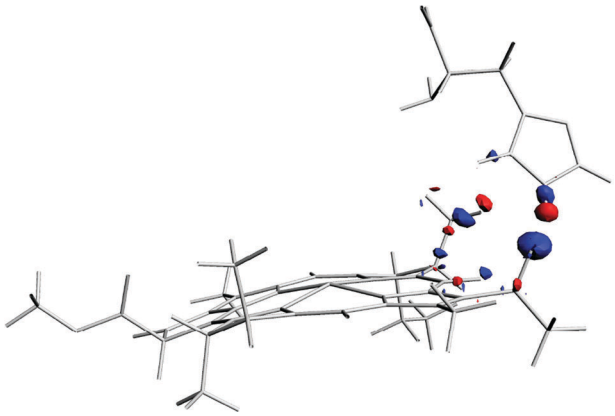

Fig. 3 Change in the electronic density upon P_L–His L168 hydrogen bond formation. The isosurface value is 0.0012 e $Å^{-3}$. Red corresponds to an increase of the density, as compared to the separated BChl *a* and His fragments, while blue denotes a decrease in the electronic density.

Table 1 Sum of quadrupole derived charges for P_L and P_M in various models

Model	q^{PL}	q^{PM}
Model 1—P	0.08	−0.08
Model 2—P + side	0.06	−0.08
Model 3—P + side + Asn	0.07	−0.08
Model 4—P + axial	−0.02	−0.21
Model 5—P + axial + H_2O(L)	−0.01	−0.23
Model 6—P + axial + H_2O(M)	−0.01	−0.22
Model 7—P + axial + side	−0.02	−0.18
Model 8—P + axial + side + Asn + H_2O(L) + H_2O(M)	−0.02	−0.19

Table 2 Orientation of the axial histidines with respect to ligated BChl *a* in the special pair. The <BH corresponds to the dihedral angle between the C_γ–C_δ–N_τ and N_I–N_{II}–N_{III} planes. See Scheme 1 for the atom labeling

	His L173	His M202
<BH	78°	88°
C_δ–N_τ–Mg	122°	128°
N_I–Mg–N_τ–C_δ	−135°	−151°

Table 3 Sum of quadrupole derived charges for P_L and P_M in various models of the special pair. The φ_{ac} corresponds to the C4–C3–$C3^1$–$O3^1$ dihedral angle and the φ_{met} to the C4–C3–$C3^1$–$C3^2$ dihedral angle of P_L

Model	φ_{ac}	φ_{met}	q^{PL}	q^{PM}
Model 1	92°	−137°	0.08	−0.08
Model 9	40°	−138°	0.05	−0.05
Model 10	−173°	11°	0.00	0.00

P_L more positively charged. However, as can be seen in Fig. 3, the hydrogen bonding induces only a small charge polarization with an increase in electronic density between N_τ and $O3^1$, but no clear net charge transfer. In Fig. 3 we can also observe the steric interaction with $C7^1$ methyl which can contribute to the asymmetric change.

Axial histidines have a larger effect on the electronic density and enhance the original asymmetry of the special pair, having a different effect on the two bacteriochlorophylls *a*.[33] Specifically in model **4**, His L173 donates a charge of 0.10 e to P_L, while His M202 donates a charge of 0.13 e to P_M (Table 1). The charge transfer from those axial histidines is essentially of the same nature as observed for the LH2 complex,[34] and it also depends on the relative distance and orientation of His and BChl *a*. A closer look at the orientation of the two histidines reveals that His M202 has its imidazole ring almost perpendicular to the bacteriochlorophyll *a* plane and slightly more tilted, contrary to His L173 (Table 2). Moreover the two histidines appear to be rotated differently around the Mg–N_τ axis.

The next two models in Table 1, namely models **5** and **6**, contain a single water molecule hydrogen bonded to one of the axial histidines. We can see that the water has also a small effect, increasing slightly the asymmetry of the special pair. It is also observed that a hydrogen bond between a water molecule and the N_π atom of axial histidine has a small effect on the histidine orientation with respect to the bacteriochlorophyll *a* molecule. Therefore, it can be concluded that the distinct orientation of the two axial histidines is a consequence of geometrical and steric adjustments to optimize the hydrogen bonding network with the proximal protein environments, including the two water molecules. Finally, by looking at the total charges in the models **7** and **8** containing the special pair, axial and side residues, it is visible that the side residues have some polarization effect and in the largest model **8** the asymmetry between P_L and P_M is about 0.17 electron, very similar in the absolute value to the asymmetry of the special pair only. The axial histidines shift the total charges for P_L and P_M by ~0.1 e. The data presented in Table 1 show that P_M has more electron charge density than P_L in the ground state. Our finding that the special pair carries a net negative charge of ~0.2 e is consistent with SSNMR data in the ground state.[8,15,16] We can also clearly conclude that this excess negative charge is mostly due to a charge transfer from the axial histidines and that the hydrogen bonded His L168 has only a minor effect. However the SSNMR data suggest an accumulation of electron charge mostly on the pyrrole ring I of P_L and less on P_M. This appears to be in contrast with our results, although one should take into account that here we are calculating the total charge on the BChls *a*, while the NMR chemical shift data are available only for a limited set of carbon atoms. Indeed if we consider only the C atoms in evaluating the relative charge of the two BChls *a* in our model, the overall picture can qualitatively change.

As discussed above, the special pair exhibits an intrinsic electronic asymmetry that reflects its geometry and apparently affects the electronic structure and the chemical shifts of the coordinating histidines.[33] Comparing P_L and P_M bacteriochlorophylls *a*, it is noticeable that the 3^1 acetyl group has substantially different orientation in the two molecules. Each of the 3^1 acetyl groups of the special pair may be oriented either with the oxygen facing outward and forming a hydrogen bond to the surrounding protein, or with the oxygen pointing inward and acting as a sixth ligand to the magnesium of the other BChl *a*.[35] There is a competition between a high conjugation with the porphyrin ring in a co-planar acetyl geometry and optimization of the electrostatic intermolecular interactions and steric repulsion in a more twisted acetyl orientation. For P_M the acetyl group is almost co-planar with the BChl *a* and thus highly conjugated with the porphyrin electronic structure, while for P_L the acetyl is out of plane and less conjugated. The electronic asymmetry of the special pair vanishes when the P_L acetyl group is forced almost in the plane of bacteriochlorophyll *a* (Table 3, model **10**). Fig. 4 and 5 confirm that when the acetyl of P_L bacteriochlorophyll *a* lies in plane, hardly any electron density difference is observed between the P_L and P_M, while when the acetyl is out of plane,

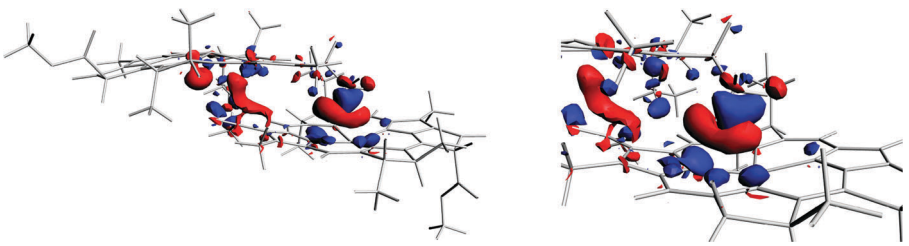

Fig. 4 Change in the electronic density upon P_L–P_M dimer formation in model **1**. The isosurface value is 0.0012 e $Å^{-3}$. Red corresponds to an increase of the density in the complex, as compared to the separated BChl *a* fragments, while blue denotes a decrease in the electronic density. The right panel shows the P_L acetyl area in detail.

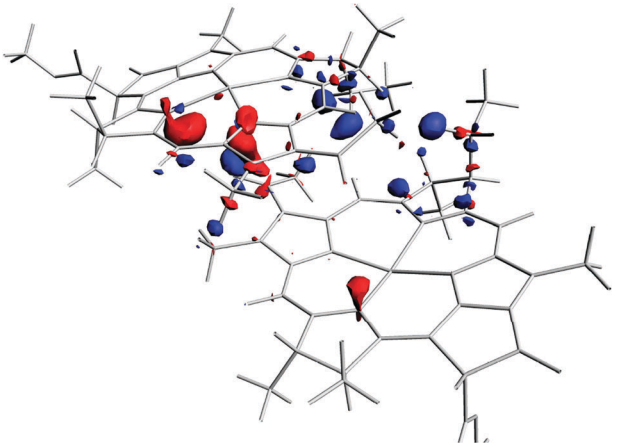

Fig. 5 Change in the electronic density upon P_L–P_M dimer formation for model **10** (with planar P_L acetyl). The isosurface value is 0.0012 e Å^{-3}. Red corresponds to an increase of the density in the complex, as compared to the separated BChl *a* fragments, while blue denotes a decrease in the electronic density.

Table 4 Orientation of the 3^1 acetyl group in single BChl *a* models. The φ_{ac} corresponds to the C4–C3–C3^1–O3^1 dihedral angle and the φ_{met} to the C4–C3–C3^1–C3^2 dihedral angle of P_L

Model	φ_{ac}	φ_{met}
Model 11—optimized BChl *a*	0°	180°
Model 12—optimized BChl *a*	−179°	1°
Model 13—P_L	27°	−151°
Model 14—P_L + His L168	47°	−132°

the perturbation is large.[11] The bulky C3^2 methyl group of the P_L acetyl penetrates the electronic cloud of the P_M bacteriochlorophyll *a* inducing a strong electronic polarization. This geometry is similar to the geometry observed for the Zinc chlorin aggregates, where it was found that the self-assembly can be driven mostly by electrostatic and van der Waals interactions without hydrogen bonding.[18]

This acetyl orientation may be influenced by the presence of the hydrogen-bonded His L168, as presented in Table 4. For the optimized bacteriochlorophyll *a* there are two in-plane acetyl conformations: In one conformer the acetyl oxygen is located on the side of the C4 atom, while in the other is pointing towards the C2^1 methyl group. It was found that the first is lower in energy by 4 kcal mol^{-1}. When the P_L bacteriochlorophyll *a* is extracted from model **1** and its acetyl optimized, the φ_{ac} angle drops down to 27°, while if the same optimization is performed in the presence of His L168, the angle settles at 47°. Similar calculations performed for various special pair models do not provide a clear picture, as for the special pair the situation is more complex due to multiple steric, π–π, and electrostatic effects, particularly a competition between the P_L–His L168 hydrogen bond and Mg–O attraction. However, it is known that the formation of the hydrogen bond to His L168 forces the acetyl group of P_L to rotate out of the molecular plane.[36] Various X-ray crystallography structures report quite different values for the acetyl angle in the range between −2° and 21°.[20] Therefore at room temperature the acetyl group most likely samples a large range of orientations and first principles molecular dynamics simulations would be more appropriate here to get a reliable statistical average of this parameter. When the hydrogen bond between His L168 and P_L is removed or its strength is altered by mutations, a change in the electron transfer kinetics is observed.[37–39]

3.2 Absorption properties

Bacteriochlorophyll *a* has two major absorption bands, usually referred to as Q_x and Q_y.[1] The most intense Q_y band appears in the region 750–800 nm and the less intense Q_x band between 550 and 600 nm. Table 5 presents the computed TDDFT absorption spectra for the optimized BChl *a* monomer, P_L and P_M extracted from model **1**, P_L + His L173 and P_M + His M202 from model **4**, and for P_L with the 3^1 acetyl group in plane (model **10**).

First of all we note that the TDDFT calculated absorption bands for the optimized monomer (Opt BChl *a*) are in perfect agreement with recently published TDDFT calculations[40] and reproduce reasonably well the experimental values for the low-lying excitations, although they underestimate the energy difference between the Q_y and the Q_x: specifically the Q_y peak is overestimated by ≈0.15 eV while the Q_x peak is underestimated by ≈0.15 eV. These deviations are within the typical TDDFT error due to the approximation in the exchange-correlation functional and are not of much concern in this work since we are interested mostly in trends and not in the exact values. The analysis of the TDDFT results shows that the dominant contribution to the Q_y absorption peak is the HOMO → LUMO transition, while the Q_x band has a strong HOMO − 1 → LUMO character mixed with the HOMO → LUMO + 1 to a less extent. This molecular orbitals analysis is consistent with earlier semi-empirical calculations.[41]

Fig. 6 shows the energy of the most relevant molecular orbitals for a fully optimized bacteriochlorophyll *a*, as well as for P_L and P_M, extracted from model **1**. Interestingly, the HOMO is higher in energy in P_L than in P_M, while the LUMO is lower in P_M than in P_L. The differences in molecular orbital energies and in the total binding energy compared with the optimized bacteriochlorophyll *a* indicate considerable distortions for the two BChls *a* in the special pair. A useful quantity that can be extracted from these results is the redox asymmetry E_0, for which a reliable experimental estimate of 0.069 eV can be found in the literature.[42] We can roughly estimate this quantity by taking the difference between the HOMO orbital energies of P_L and P_M: if we use the geometry of P_L and P_M extracted from model **1**, we obtain E_0 = 0.22 eV (see also Fig. 6),

Table 5 Main absorption peaks computed with TDDFT for several models including a single BChl *a*. Values are given in nm

Model	Q_x	Q_y
Opt BChl *a*	617	703
P_M model **1**	612	712
P_M + His M202 model **4**	633	716
P_L Model **1**	571	666
P_L + His L173 model **4**	600	670
P_L model **10**	594	695

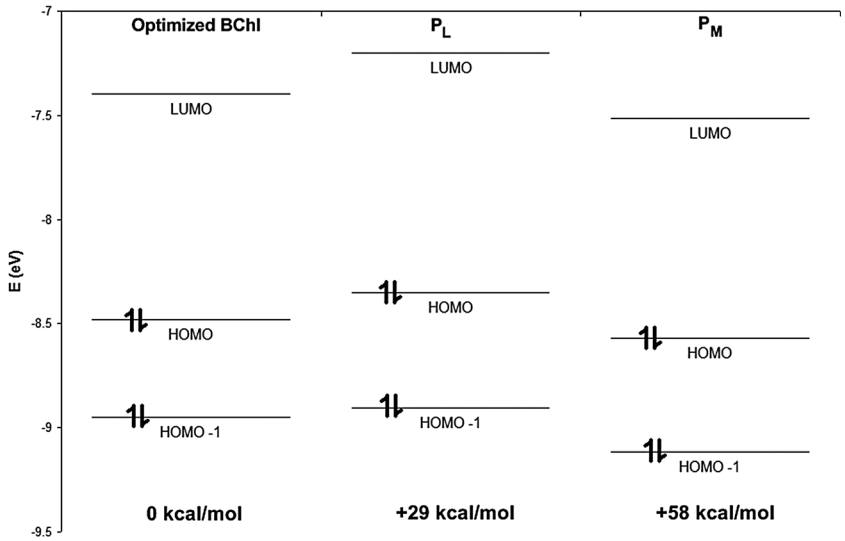

Fig. 6 Energy levels and total bonding energies of P_L, P_M (from model **1**) compared to the optimized bacteriochlorophyll *a*.

while for model **10** (acetyl almost in plane) we find $E_0 = 0.05$ eV, which is closer to the experimental value. This estimate takes into account only the asymmetry originating from conformational differences of the BChls, but does not include long-range electrostatic effects due to the surrounding protein. For P_L + His L173 and P_M + His M202, both extracted from model **4**, the picture is similar (Fig. 7) with the HOMO being higher in energy in P_L and the LUMO being lower in P_M. These results already qualitatively indicate that a considerable charge transfer character should be expected in the excited state of P, with electronic charge moving from P_L to P_M. A $P_L^+P_M^-$ charge transfer state has been indeed suggested on the basis of absorption and Stark spectroscopy.[14,43]

From the comparison of the main absorption peaks in Table 5 we can see how the geometrical distortions and the axial histidine affect the excitation energies, neglecting for the moment the effect of the coupling between P_L and P_M. The absorption spectrum of P_M is very similar to that of the optimized BChl *a*, while in the spectrum of P_L the two major bands Q_x and Q_y are strongly blue-shifted by about 35 nm. This shift can be rationalized on the basis of the strong out of plane orientation of the acetyl group. In fact, when the 3^1 acetyl group is rotated into the plane of P_L bacteriochlorophyll *a* and optimized (model **10**), the spectrum bands shift closer to the positions of the optimized BChl *a*. The shift in Q_y band between P_L of model **1** and P_L of model **10** is consistent with ref. 41. Therefore the orientation of the acetyl has a large influence on the electronic structure and optical properties of the whole bacteriochlorophyll *a*. When the 3^1 acetyl group is in the porphyrin plane, the electronic conjugation of the main ring extends to the acetyl, while when the acetyl group is out of plane, the conjugation weakens. For both P_L and P_M,

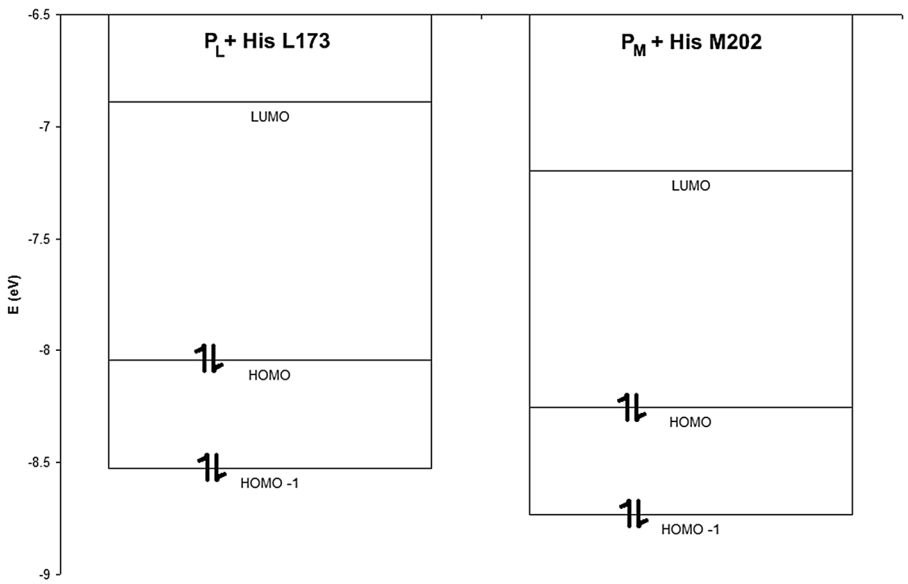

Fig. 7 Energy levels of P_L + His L173 and P_M + His M202 from model **4**.

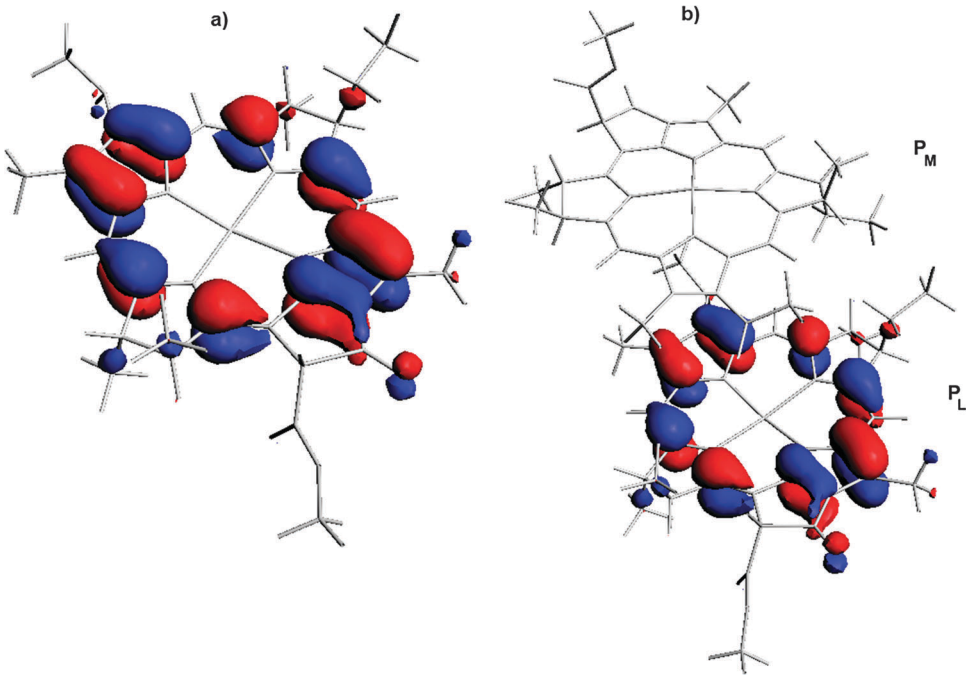

Fig. 8 HOMO of P_L (a) and P (b).

the addition of axial histidines induces a red-shift for both bands and especially for the Q_x absorption.

The effect of electronic coupling in the BChl *a* dimer of the BRC special pair is illustrated with Fig. 8, which shows the HOMO of P in comparison with the HOMO of P_L extracted from model **8**. Clearly in this conformation the HOMO of P is almost entirely localized on P_L and is hardly affected by the dimer formation. This strong localization of the HOMO is in contrast with electron spin resonance data showing that the ensemble average of the electron spin density in the radical cation state is delocalized on the two BChls *a* of P.[44,45] Also the recent photo-CIDNP data show an average electron spin density distribution between P_L and P_M of about 70 : 30 in favor of P_L.[16] The localization of the HOMO in the model **8** can be associated to the out of plane rotation of the acetyl group having a destabilizing effect on the HOMO of P_L with respect to the HOMO of P_M (see also Fig. 6). However, when the P_L 3^1 acetyl group is rotated into the plane of bacteriochlorophyll *a* (model **10**) then both the HOMO and LUMO appear to be more delocalized onto the whole special pair (see Fig. 9). Rotation of the acetyl group to a configuration close to planar increases the symmetry of the two fragments of the special pair and brings the HOMO of P_L and HOMO of P_M closer in energy, as presented in Fig. 10. Nevertheless, as can be seen in Fig. 9, the HOMO has a larger localization on P_L, while the LUMO is more localized on P_M, indicating that a partial charge transfer character in the Q_y excitation is still present as suggested by experimental data.[14,43]

The same calculations repeated for the special pair extracted from the 1QOV structure, which has the acetyl dihedral angle smaller, lead to similar results. Consistently with model **10**, the HOMO and LUMO orbitals were found to be delocalized over the entire special pair, but with the HOMO (LUMO) having more weight on P_L (P_M), respectively. The total quadrupole

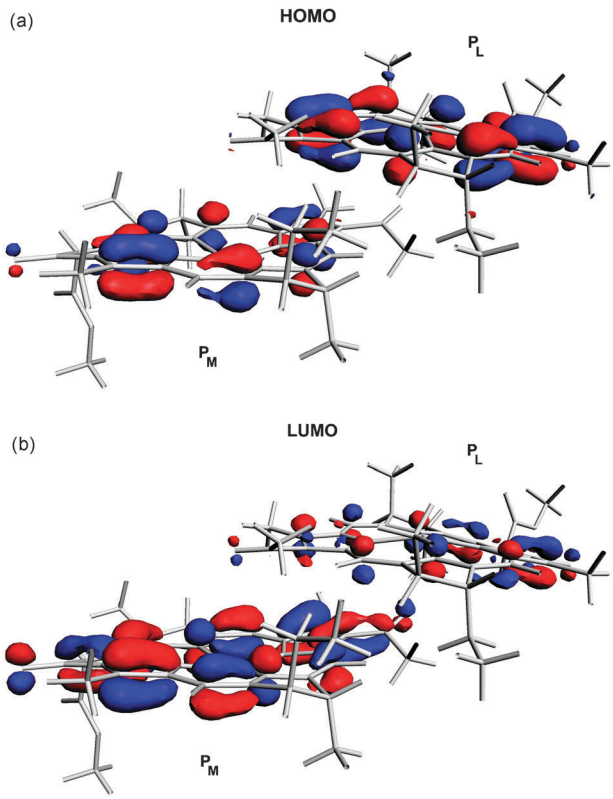

Fig. 9 HOMO and LUMO of special pair from model **10**.

derived charges for P_L and P_M were 0.03 and −0.03, respectively. Thus, also the model of P extracted from the 1QOV structure shows an asymmetric charge distribution with P_M being more negatively charged. We can conclude that models derived from different crystallographic structures are qualitatively

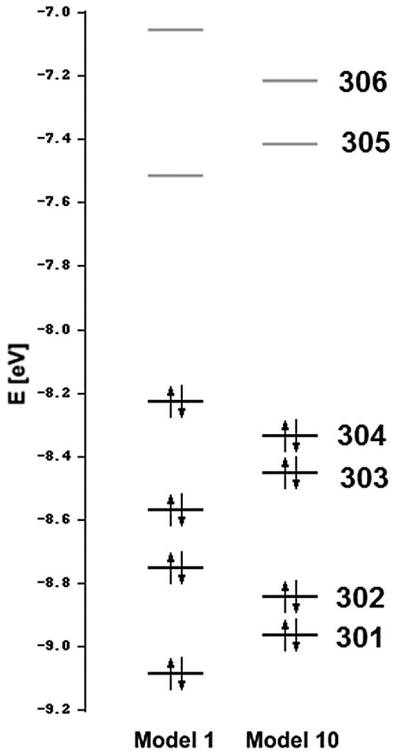

Fig. 10 Orbital energies in special pair from models **1** and **10**.

consistent with each other, although quantitative differences are observed mostly due to the different acetyl orientation on P_L.

The absorption spectra for various models are presented in Fig. 11. It is evident that the Q_y band is now split due to exciton coupling in the special pair. The absorption bands consist now of several transitions with different weights as shown for model **1**. Within the supermolecule approach used here, any monomeric excited state splits into two excited states upon chromophore dimerization, each with a different energy and transition dipole moment, as a direct result of exciton coupling and possibly also interchromophore charge transfer. An estimate of the exciton coupling can be obtained as the difference between the first two excitation energies. For model **1** we obtain an exciton coupling of 0.07 eV. The Q_y band splitting is only slightly increased when including the three histidines and phenylalanine (model **7**). In the model **10** containing the P_L 3^1 acetyl group rotated into the plane of bacteriochlorophyll *a*, the exciton coupling is reduced to 0.04 eV. The low-energy absorption band of the BRC is at 890 nm at 15 K and increases in energy to 860 nm at room temperature.[46] If one takes the 800 nm absorption of the monomeric BChl *a* as the value of the wavelength, at which the special pair would absorb without the pigment–pigment coupling, the shift to 890 nm corresponds to an energy shift of $\sim$0.15 eV. Thus, the present TDDFT calculations strongly underestimate the exciton coupling. There might be several reasons for this discrepancy, including the approximation in the functional, the neglect of long range interactions with the protein, a poor description of contributions due to charge transfer states. A detailed investigation of all these effects is beyond the scope of the present work. We refer to a recent paper by Thomas Renger and coworkers for a detailed analysis of the exciton coupling in BRC based on an effective two-state model Hamiltonian.[47]

4. Discussion and conclusions

It has been recently discovered that protein dynamics drives the first steps in photosynthetic charge separation.[48,49] However, taking into account that the primary electron transfer happens on a very short time scale of $\sim$3 ps, there is not much time for the protein to undergo large rearrangements. Certainly, 3 ps is enough to move one or even several protons around, leading to the concept of a proton-coupled electron transfer (PCET), where the transfer of a proton assists the electron transfer. It has been reported that the water molecule between His M202 and B_A is important for optimization of the primary electron transfer rate and that steric exclusion of that water in a mutant generates *ca.* an 8-fold decrease in the decay rate of the P* state.[50] Moreover, a hydrogen bond between the water molecule and the 13^1 carbonyl of B_A is observed in the oxidized special pair $P^{+\bullet}$ but deemed weak or nonexistent in the special pair neutral ground state. It is also suggested that a possible through-bond connection between the special pair and B_A facilitated by His M202 and the water molecule may exist.[33,50,51] If the proton transfer, or just a shift in the hydrogen bond equilibrium had to occur first between His M202 and the associated water molecule, that histidine would gain partially anionic character and it would be stabilized by the presence of the magnesium ion. This would in turn change the relative geometry of His and BChl *a*, including shortening of the Mg–N distance, and induce a larger charge transfer to the special pair. Interestingly, P_M is found to have more electronic charge than P_L in the ground and excited state.[14] The additional negative charge would facilitate the electron transfer from P*. On the electron acceptor, B_A, the 13^1 carbonyl is conjugated to the π electron system of its porphyrin ring. Therefore formation of a hydrogen bond with the water molecule (or H_3O^+) provides an opportunity to fine-tune the redox potential, making the accessory bacteriochlorophyll *a* easier to reduce and lowering the free energy of the $P^+B^-_A$ state. All together this would facilitate the electron transfer from P* to B_A. In order to stabilize the positive charge on the special pair and to prevent charge recombination, the 3^1 acetyl of P_L could be rotated if enough driving force is available to break the hydrogen bond with His L168. Such a rotation will alter the electronic structure of the bacteriochlorophyll *a* dimer. Molecular dynamics simulations suggest that the acetyl rotates on oxidation, while coupled-cluster calculations on gas-phase energetics of that process indicate that *ca.* 7 kcal mol^{-1} driving force is provided by the preference of the charged BChl *a* Mg to be coordinated to the carbonyl rather than to the methyl group.[33,52,53] This energy is enough to break the hydrogen bond between P_L and His L168. In that respect the acetyl group would act as a valve to protect the system from fast charge recombination. In all known reaction centers an electron moves at least one step down to acceptor chain before the oxidized primary donor is reduced.

The possibility of the above-mentioned through-bond connection between the primary electron donor and acceptor,

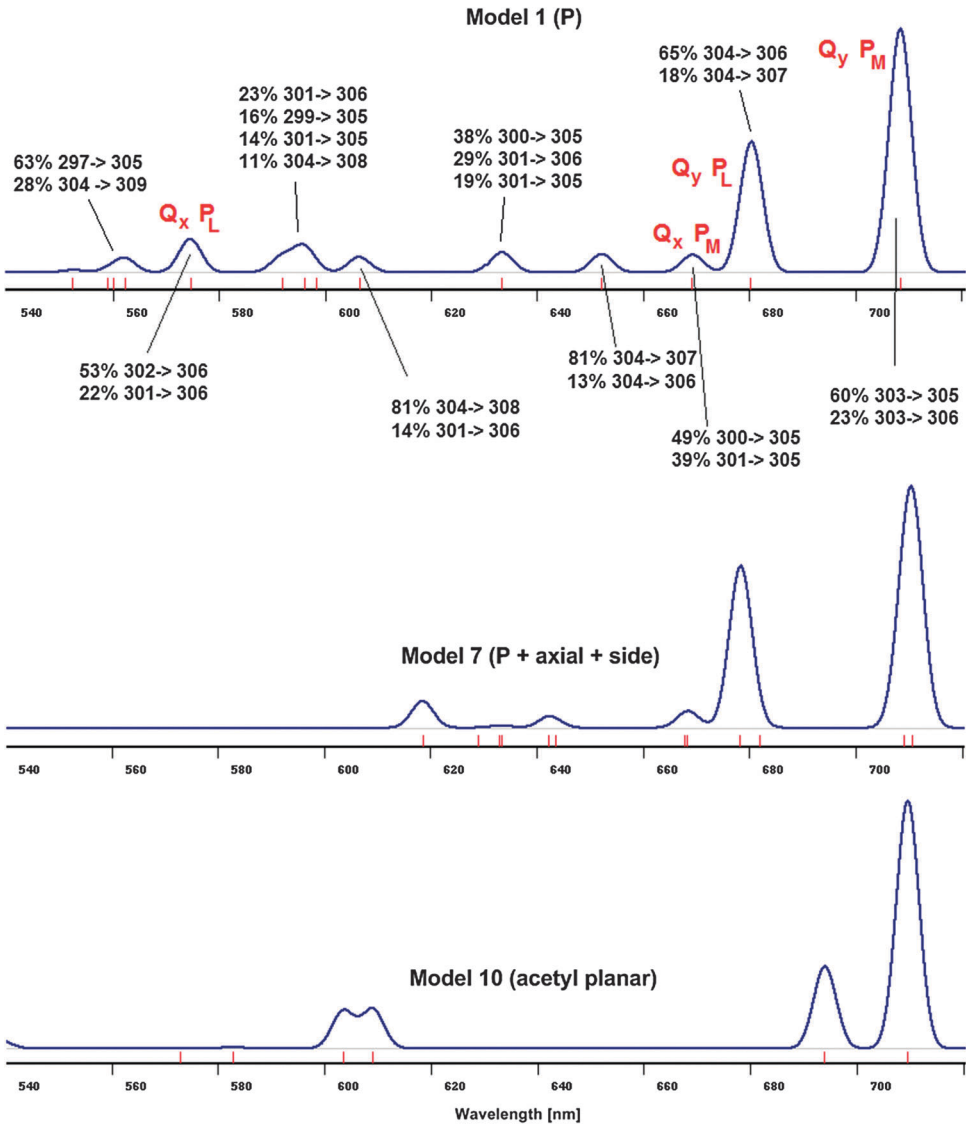

Fig. 11 TDDFT absorption spectra of special pair models. The main contributions to the bands are indicated. Note that 304 is HOMO and 305 LUMO. The numbers indicate orbitals that mostly contribute to the transitions.

the speculated proton transfer, and the 3^1 acetyl rotation to block recombination of the cation radical are intriguing suggestions that should be further explored. Particularly a thorough investigation of the acetyl rotation profile and constraints, as well as the associated impact on the electronic structure of P before and after the primary electron transfer should be pursued. Finally, possible proton transfer paths should be addressed by employing more extensive models within a QM/MM approach.

An analysis of the electron charge difference between P_L and P_M bacteriochlorophylls *a* of the special pair was presented, together with a TDDFT study of the absorption properties. It is found that the electron asymmetry is an intrinsic feature of the special pair and is strongly modulated by the specific orientation of the 3^1 acetyl group, which is hydrogen bonded to His L168. Since the acetyl group can conjugate to the π electron system of BChl *a*, and this conjugation decreases in strength as the carbonyl group is rotated out of the macrocycle plane, the protein can tune the biophysical properties of the special pair by enforcing conformational changes to the acetyl. If its orientation is close to the plane of P_L, the electron density perturbation in the special pair and consequently the observed asymmetry is strongly reduced. These changes are also reflected in the absorption spectra and in the localization of the relevant molecular orbitals. When the acetyl is oriented out of plane, significant blue shifts for the main absorption bands of bacteriochlorophyll *a* are predicted.

Although crystallographic data do not provide a precise determination of the acetyl rotation, we can draw some conclusions that are valid for models with different acetyl group orientation: (i) both P_L and P_M BChl *a* carry a negative charge due primarily to electron charge donation by the axial histidines; (ii) the ground state electronic density is asymmetric with P_M being more negatively charged than P_L; (iii) the HOMO to LUMO electronic transition has a partial charge transfer character with electron charge moving from P_L to P_M in agreement with experimental data in the excited state;[14] (iv) increased dihedral angle for the acetyl group rotation enhances electronic asymmetry of the special pair and decreases delocalization of the molecular orbitals.

Acknowledgements

This work was supported by the Netherlands Organization for Scientific Research (NWO) via the Top Grant on 'Ultrahigh field solid-state NMR of photosynthesis and artificial photosynthetic energy conversion systems'. The use of supercomputer facilities was sponsored by The Netherlands National Computing Facilities Foundation (NCF), with financial support from NWO.

References

1 R. E. Blankenship, *Molecular Mechanisms of Photosynthesis*, Wiley-Blackwell Science Ltd, Oxford, 2002.
2 J. Deisenhofer and H. Michel, *Highresolution crystal structures of bacterial photosynthetic reaction centers*, in *Molecular Mechanisms in Bioenergetics*, ed. L. Ernster, Elsevier Science Publishing, Amsterdam, 1992, pp. 103–120.
3 B. A. Heller, D. Holten and C. Kirmaier, *Science*, 1995, **269**, 940.
4 W. Holzapfel, *et al*., *Proc. Natl. Acad. Sci. U. S. A*., 1990, **87**, 5168.
5 S. Lin, E. Katilius, A. L. M. Haffa, A. K. W. Taguchi and N. W. Woodbury, *Biochemistry*, 2001, **40**, 13767.
6 J. P. Allen, J. M. Cordova, C. C. Jolley, T. A. Murray, J. W. Schneider, N. W. Woodbury, J. C. Williams, J. Niklas, G. Klihm, M. Reus and W. Lubitz, *Photosynth. Res*., 2009, **99**, 1.
7 P. Kanchanawong, M. G. Dahlbom, T. P. Treynor, J. R. Reimers, N. S. Hush and S. G. Boxer, *J. Phys. Chem. B*, 2006, **110**, 18688.
8 S. Prakash, A. Alia, P. Gast, H. J. M. de Groot, G. Jeschke and J. Matysik, *Biochemistry*, 2007, **46**, 8953.
9 H. Yamasaki, H. Nakamura and Y. Takano, *Chem. Phys. Lett*., 2007, **447**, 324.
10 H. Yamasaki, Y. Takano and H. Nakamura, *J. Phys. Chem. B*, 2008, **112**, 13923.
11 F. Lendzian, M. Huber, R. A. Isaacson, B. Endeward, M. Plato, B. Bönigk, K. Möbius, W. Lubitz and G. Feher, *Biochim. Biophys. Acta*, 1993, **1183**, 139.
12 J. Rautter, F. Lendzian, W. Lubitz, S. Wang and J. P. Allen, *Biochemistry*, 1994, **33**, 12077.
13 W. Lubitz, F. Lendzian and R. Bittl, *Acc. Chem. Res*., 2002, **35**, 313.
14 L. J. Moore, H. L. Zhou and S. G. Boxer, *Biochemistry*, 1999, **38**, 11949.
15 E. A. M. Schulten, J. Matysik, A. Alia, S. Kiihne, J. Raap, J. Lugtenburg, P. Gast, A. J. Hoff and H. J. M. de Groot, *Biochemistry*, 2002, **41**, 8708.
16 E. Daviso, S. Prakash, A. Alia, P. Gast, J. Neugebauer, G. Jeschke and J. Matysik, *Proc. Natl. Acad. Sci. U. S. A*., 2009, **106**, 22281.
17 H. Treutlein, K. Schulten, A. T. Brunger, M. Karplus, J. Deisenhofer and H. Michel, *Proc. Natl. Acad. Sci. U. S. A*., 1992, **89**, 75.
18 S. Ganapathy, S. Sengupta, P. K. Wawrzyniak, V. Huber, F. Buda, U. Baumeister, F. Würthner and H. J. M. de Groot, *Proc. Natl. Acad. Sci. U. S. A*., 2009, **106**, 11472.
19 U. Ermler, G. Fritzsch, S. K. Buchanan and H. Michel, *Structure (London)*, 1994, **2**, 925.
20 D. Spiedel, A. W. Roszak, K. McKendrick, K. E. McAuley, P. K. Fyfe, E. Nabedryk, J. Breton, B. Robert, R. J. Cogdell, N. W. Isaacs and M. R. Jones, *Biochim. Biophys. Acta*, 2002, **1554**, 75.
21 K. E. McAuley, P. K. Fyfe, J. P. Ridge, N. W. Isaacs, R. J. Cogdell and M. R. Jones, *Proc. Natl. Acad. Sci. U. S. A*., 1999, **96**, 14706.
22 G. te Velde, F. M. Bickelhaupt, S. J. A. van Gisbergen, C. Fonseca Guerra, E. J. Baerends, J. G. Snijders and T. Ziegler, *J. Comput. Chem*., 2001, **22**, 931.
23 C. Fonseca Guerra, J. G. Snijders, G. te Velde and E. J. Baerends, *Theor. Chem. Acc*., 1998, **99**, 391.
24 ADF2007.01, SCM, Theoretical Chemistry, Vrije Universiteit, Amsterdam, The Netherlands, http:// www.scm.com.
25 A. D. Becke, *Phys. Rev. A*, 1988, **38**, 3098.
26 C. T. Lee, W. T. Yang and R. G. Parr, *Phys. Rev. B: Condens. Matter*, 1988, **37**, 785.
27 B. Miehlich, A. Savin, H. Stoll and H. Preuss, *Chem. Phys. Lett*., 1989, **157**, 200.
28 F. Buda, H. J. M. de Groot and A. Bifone, *Phys. Rev. Lett*., 1996, **77**, 4474.
29 M. Swart, P. Th. van Duijnen and J. G. Snijders, *J. Comput. Chem*., 2001, **22**, 79.
30 P. R. T. Schipper, O. V. Gritsenko, S. J. A. van Gisbergen and E. J. Baerends, *J. Chem. Phys*., 2000, **112**, 1344.
31 O. V. Gritsenko, P. R. T. Schipper and E. J. Baerends, *Chem. Phys. Lett*., 1999, **302**, 199.
32 O. V. Gritsenko, P. R. T. Schipper and E. J. Baerends, *Int. J. Quantum Chem*., 2000, **76**, 407.
33 A. Alia, P. K. Wawrzyniak, G. J. Janssen, F. Buda, J. Matysik and H. J. M. de Groot, *J. Am. Chem. Soc*., 2009, **131**, 9626.
34 P. K. Wawrzyniak, A. Alia, R. G. Schaap, M. M. Heemskerk, H. J. M. de Groot and F. Buda, *Phys. Chem. Chem. Phys*., 2008, **10**, 6971.
35 J. M. Hughes, M. C. Hutter, J. R. Reimers and N. S. Hush, *J. Am. Chem. Soc*., 2001, **123**, 8550.
36 J. Rautter, F. Lendzian, C. Schulz, A. Fetsch, M. Kuhn, X. Lin, J. C. Williams, J. P. Allen and W. Lubitz, *Biochemistry*, 1995, **34**, 8130.
37 H. A. Murchison, R. G. Alden, J. P. Allen, J. M. Peloquin, A. K. W. Taguchi, N. W. Woodbury and J. C. Williams, *Biochemistry*, 1993, **32**, 3498.
38 T. A. Mattioli, J. C. Williams, J. P. Allen and B. Robert, *Biochemistry*, 1994, **33**, 1636.
39 A. Ivancich, T. A. Mattioli, K. Artz, S. Wang, J. P. Allen and J. C. Williams, *Biochemistry*, 1997, **36**, 3027.
40 J. Neugebauer, *J. Phys. Chem. B*, 2008, **112**, 2207.
41 E. Gudowska-Nowak, M. D. Newton and J. Fajer, *J. Phys. Chem*., 1990, **94**, 5795.
42 J. R. Reimers and N. S. Hush, *J. Am. Chem. Soc*., 2004, **126**, 4132.
43 D. J. Lockhart and S. G. Boxer, *Proc. Natl. Acad. Sci. U. S. A*., 1988, **85**, 107.
44 J. R. Norris, R. A. Uphaus, H. L. Crespi and J. J. Katz, *Proc. Natl. Acad. Sci. U. S. A*., 1971, **68**, 625.
45 J. R. Norris, H. Scheer, M. E. Druyan and J. J. Katz, *Proc. Natl. Acad. Sci. U. S. A*., 1974, **71**, 4897.
46 H. Huber, M. Meyer, M. Scheer, W. Zinth and J. Wachtveitl, *Photosynth. Res*., 1998, **55**, 153.
47 M. El-Amine Madjet, F. Muh and T. Renger, *J. Phys. Chem*., 2009, **113**, 12603.
48 H. Wang, S. Lin, J. P. Allen, J. C. Williams, S. Blankert, C. Laser and N. W. Woodbury, *Science*, 2007, **316**, 747.
49 H. Lee, Y. C. Cheng and G. R. Fleming, *Science*, 2007, **316**, 1462.
50 J. A. Potter, P. K. Fyfe, D. Frolov, M. C. Wakeham, R. van Grondelle, B. Robert and M. R. Jones, *J. Biol. Chem*., 2005, **280**, 27155.
51 P. K. Wawrzyniak, H. J. M. de Groot and F. Buda, *Photosynth. Res*., submitted.
52 I. Muegge, J. Apostolakis, U. Ermler, G. Fritzsch, W. Lubitz and E. W. Knapp, *Biochemistry*, 1996, **35**, 8359.
53 J. Apostolakis, I. Muegge, U. Ermler, G. Fritzsch and E. W. Knapp, *J. Am. Chem. Soc*., 1996, **118**, 3743.